A circular RNA derived from MMP9 facilitates oral squamous cell carcinoma metastasis through regulation of MMP9 mRNA stability

Bing Xia[1], Tao Hong[1] ⑩, Xin He[1], Xinlan Hu[1], and Yongbo Gao[1]

Abstract

Emerging evidence demonstrates that dysregulation of circular RNA is linked to tumorigenesis and aggressive progression. However, its role in oral squamous cell carcinoma remains largely uncharacterized. In this study, we identified a novel metastasis-associated circular RNA, circular matrix metalloproteinase 9 (hsa_circ_0001162, a circular RNA derived from matrix metalloproteinase 9), which was remarkably upregulated in oral squamous cell carcinoma and positively correlated with matrix metalloproteinase 9 expression. Patients with high circular matrix metalloproteinase 9 expression were prone to lymph node metastasis and an advanced TNM stage. Importantly, circular matrix metalloproteinase 9 was identified as an efficacious diagnostic and prognostic biomarker for oral squamous cell carcinoma patients. Functional experiments showed that depletion of circular matrix metalloproteinase 9 weakened the migratory and invasive capabilities of oral squamous cell carcinoma cells in vitro as well as inhibited lung metastasis in vivo. Regarding the mechanism, circular matrix metalloproteinase 9 could simultaneously interact with AUF1 and miR-149 to block the inhibitory effect of AUF1 and miR-149 on matrix metalloproteinase 9 3′-untranslated region, resulting in enhanced matrix metalloproteinase 9 messenger RNA stability, thereby facilitating oral squamous cell carcinoma metastasis. Collectively, our data indicate that circular matrix metalloproteinase 9 acts as a metastasis-promoting gene in oral squamous cell carcinoma through regulating the messenger RNA stability of its parental gene. Therapeutic targeting of circular matrix metalloproteinase 9 may be a promising treatment intervention for metastatic oral squamous cell carcinoma patients.

Keywords

Circular RNA, OSCC, mRNA stability, metastasis, biomarker

Introduction

Oral squamous cell carcinoma (OSCC) is the main pathological type of oral cancer (accounting for approximately 90% of cases) and the eighth most common malignant tumor worldwide[1]. It is still considered a lethal disease, especially in India and South East Asia[2]. Although great efforts have been made in the diagnosis and treatment of OSCC in recent decades, the 5-year survival rate is still very low, especially in patients with metastasis (less than 40%)[3]. Therefore, continued in-depth research into the pathogenesis of OSCC is urgently needed to provide new therapeutic interventions for patients with OSCC.

Matrix metalloproteinases (MMPs) belong to the zinc-dependent endopeptidase family and are widely distributed in the extracellular environment of various tissues. They can promote the degradation of extracellular matrix (ECM),

which enables them to participate in cancer dissemination[4]. Among them, MMP9 has been extensively studied and is highly expressed in a variety of malignant tumors, including OSCC[5]. Accumulating evidence suggests that MMP9 plays a key positive regulator in OSCC cell migration and invasion across basement membranes[6]. OSCC patients with high MMP9 expression are closely associated with metastatic

[1] Department of Stomatology, Hangzhou Red Cross Hospital, Hangzhou, China

Corresponding Author:
Tao Hong, Department of Stomatology, Hangzhou Red Cross Hospital, Hangzhou, Zhejiang, 310000, China.
Email: lixuenongdr@163.com

clinical features and worse prognosis[7]. Although the important biological functions of MMP9 have been clearly elucidated, the mechanism of its dysregulation is still unclear.

Circular RNA (circRNA) is a special type of non-coding RNA characterized by a covalently closed ring structure, which is widely expressed in eukaryotes and functions in a tissue and developmental-stage specific pattern[8]. It is generated by the tail-to-head splicing of its host gene pre-messenger RNA (mRNA)[9]. Emerging evidence shows that circRNA participates in cancer initiation, development, and progression through regulation of its host gene via different mechanisms. For instance, circ-ITGA7 localized in the cytoplasm increased ITGA7 expression via sponging miR-370-3p and inactivating the oncogenic RAS signaling pathway[10]. Circ-FLI1 located in the nucleus promoted breast cancer metastasis by epigenetic upregulation of FLI1 via coordinately regulating TET1 and DNMT1[11]. Circ-YAP was reported to negatively modulate YAP expression via suppression of Yap translation initiation[12]. These studies reveal that circRNA is a compelling regulator of its host gene in human cancer.

Here, we screened circRNAs derived from MMP9 and found that circ-MMP9 (hsa_circ_0001162) could regulate MMP9 expression in OSCC. The clinical significance, biological function, and potential mechanisms of action of circ-MMP9 have been further studied.

Materials and Methods

OSCC Tissues, Plasma and Cell Lines

A total of 74 paired OSCC and corresponding non-tumor normal tissues were collected from the Department of Stomatology, Hangzhou Red Cross Hospital. The tissues were stored in liquid nitrogen before use. None of the patients received preoperative anti-cancer treatment. All patients provided handwritten informed consent and were followed up every 3 months. We also collected plasma samples from 16 healthy control and 25 OSCC patients to detect the expression level of circ-MMP9. This study was approved by the ethics committee of Hangzhou Red Cross Hospital. OSCC cell lines including HN4, UM1, SCC-9, SCC-15, HSC-3, and CAL-27 and the normal oral keratinocyte (NOK) cells were all obtained from the Cell Bank of the Chinese Academy of Science (Shanghai, China) and routinely cultured based on the manufacturer's instructions.

Reverse Transcription and Quantitative Real-Time PCR

Total RNA was extracted by TRIzol reagent (Invitrogen, Carlsbad, CA, USA) and reverse transcribed into complementary DNA, followed by quantification of RNA expression using SYBR Green Realtime PCR Master Mix (SinoBio, Beijing, China) and calculation using a $2^{-\Delta\Delta Ct}$ method. The primer sequences used in this study are as follows:

hsa_circ_0001161: Forward: 5′-AGCTGACTCGAC-GGTGATG-3′, Reverse: 5′-GCTTGTCCCGGTCGTA

GTT-3′; hsa_circ_0060571: Forward: 5′-TCTGGAGGAA-AGGGAGGAGT-3′, Reverse: 5′-GGTGTGGTGGTGGT TGGAG-3; hsa_circ_0001162: Forward: 5′-GAGGA AAGGGAGGGAGTGGAG-3′, Reverse: 5′-AGGCTTT-CTCTCGGTACTGG-3; MMP9: Forward: 5′-ACTGTCC ACCCCTCAGAGC-3′, Reverse: 5′-CGTCGAAGA TGT TCACGTTG-3; GAPDH: Forward: 5′-GGCCTCCAA GGAGTAAGACC-3′, Reverse: 5′-AGGGGTCTACATGG-CAACTG-3.

Establishment of Stable Circ-MMP9 Knockdown Cell Lines and Cell Transfection

The sequence targeting the circ-MMP9 junction site was inserted into PLCDH-ciR lentiviral vector (Geneseed, Guangzhou, China). The vector was then infected into OSCC UM1 and HSC-3 cells using Envirus™ enhancement reagent (Engreen, Auckland, NZ), followed by selection using puromycin for 3 days. For transient transfection, AUF1 siRNA (RiboBio, Guangzhou, China), miR-149 mimics and inhibitors (GenePharma, Shanghai, China), and MMP9 pcDNA3.1 expression plasmid (Invitrogen, Carlsbad, CA, USA) were transfected into UM1 and HSC-3 cells using Lipofectamine 3000 (Invitrogen, Carlsbad, CA, USA) in accordance with the manufacturers' protocols.

Western Blot

Total protein was isolated and transferred onto a polyvinylidene difluoride membrane, followed by blocking using defatted milk powder and incubation with corresponding primary and secondary antibodies. The membrane was then visualized using enhanced chemiluminescence solution (Beyotime, Beijing, China). The primary antibodies used were: anti-MMP9 (1:1000 dilution, #13667, CST, Danvers, MA, USA); anti-AUF1 (1:5000 dilution, #12382, CST, Danvers, MA, USA); and anti-GAPDH (1:10000 dilution, #HRP-60004, Proteintech, Rosemont, IL, USA).

Cell Migration and Invasion Assays

For migration assay, the wound was generated by using a sterile pipette tip after UM1 and HSC-3 cells grew to 80–90% confluence. After 48 hours, the wound healing area was calculated using Image J software. For the invasion assay, cells were seeded on a 24-well culture plate coated with Matrigel (BD Biosciences, San Jose, CA, USA), followed by staining and photography of cells located on the lower surface after 16 hours.

Experimental Lung Metastasis Model

A total of 18 nude mice were randomly divided into three groups (sh-NC, sh-circ-MMP9#1, and sh-circ-MMP9#2; $n=6$ per group). A total of 1×10^6 UM1 cells suspended in phosphate buffer saline (PBS) were tail-vein injected into
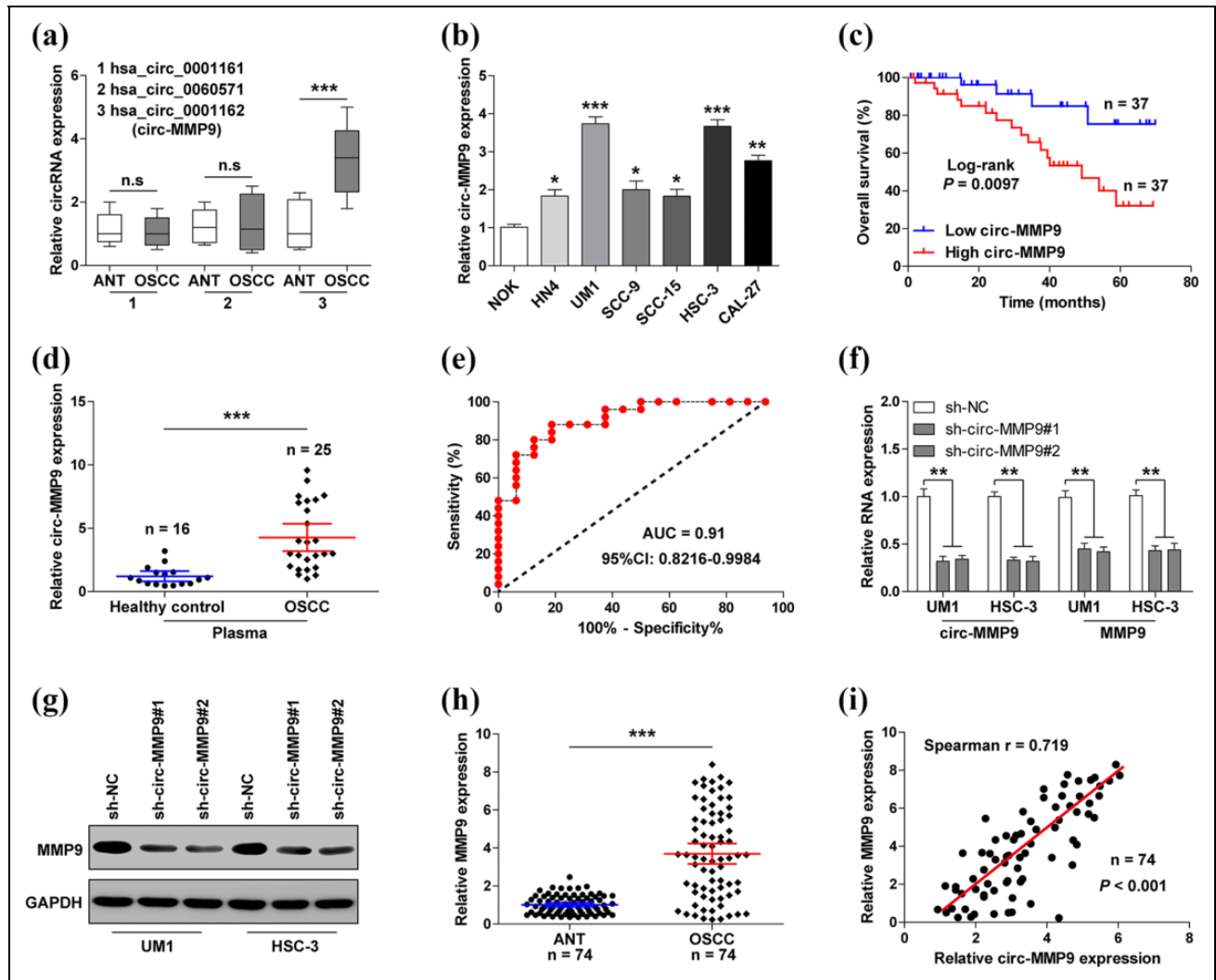
Fig 1. Circular matrix metalloproteinase 9 (circ-MMP9) is upregulated in oral squamous cell carcinoma (OSCC) and positively correlated with MMP9 expression. (a) Quantitative real-time PCR (qRT-PCR) analysis for the expression of the indicated three circRNAs in OSCC and matched normal tissues. (b) qRT-PCR analysis for circ-MMP9 expression in OSCC cell lines. (c) The survival curve of OSCC patients based on the median circ-MMP9 expression value. (d) qRT-PCR analysis for circ-MMP9 expression in plasma samples. (e) Receiver operating characteristic curve of OSCC patients based on plasma circ-MMP9 expression. (f) qRT-PCR analysis for circ-MMP9 and MMP9 expression in circ-MMP9-depleted UM1 and HSC-3 cells. (g) Western blot analysis for MMP9 protein expression circ-MMP9-depleted UM1 and HSC-3 cells. (h) qRT-PCR analysis for MMP9 expression in 74 pairs of OSCC and normal tissues. (i) The correlation between circ-MMP9 and MMP9 expression in OSCC tissues. $*p < 0.05$, $**p < 0.01$, $***p < 0.001$.

nude mice. Lung metastasis was monitored weekly using an IVIS Lumina II system. After 6 weeks, all mice were sacrificed and the lung metastasis nodules were counted. The animal study was approved by the Animal Policy and Welfare Committee of Hangzhou Red Cross Hospital.

Luciferase Reporter Assay

To evaluate the effect of circ-MMP9 on MMP9 promoter activity, the promoter sequence was subcloned into pGL3-basic luciferase vector (Promega, Madison, WI, USA), followed by transfection into circ-MMP9-depleted UM1 and HSC-3 cells. To evaluate the relationship between miR-149 and circ-MMP9/MMP9, the full-length sequences of

circ-MMP9 and MMP9 3′-untranslated region (UTR) containing the wild-type or mutant miR-149 binding site were inserted into pmirGLO vector (Promega, Madison, WI, USA). Then, the pmirGLO vectors and miR-149 mimics were co-transfected into UM1 and HSC-3 cells. The luciferase activity was detected after 48 hours of transfection by a dual-luciferase reporter system as per the standard protocols (Promega, Madison, WI, USA).

RNA Pull-down and Radioimmunoprecipitation Assay

RNA pull-down assay was performed using Pierce™ Magnetic RNA-Protein Pull-Down Kit (#20164, Thermo Fisher Scientific, Waltham, MA, USA) with biotinylated control or

circ-MMP9 probe in UM1 and HSC-3 cells, followed by Western blot analysis for AUF1 protein expression and quantitative real-time PCR (qRT-PCR) analysis for miR-183 and miR-149 expression. Radioimmunoprecipitation assay (RIPA) was carried out using RIP™ RNA-Binding Protein Immunoprecipitation Kit (Merck Millipore, Darmstadt, Germany) in accordance with the manufacturer's protocols, followed by qRT-PCR analysis for circ-MMP9 expression.

Analysis of Circ-MMP9 Localization

For nuclear-cytoplasmic fractionation assay, the cytoplasmic and nuclear RNAs were extracted and subjected to qRT-PCR analysis for circ-MMP9 expression. As internal references for cytoplasmic and nuclear fractions, 18 s and U6 were used, respectively. Fluorescence in situ hybridization (FISH) assay was performed using the FISH kit (RiboBio, Guangzhou, China) and Cy3-labed circ-MMP9 probe based on the manufacturer's manual with minor modifications.

Data Statistics

All data analysis was performed using SPSS 22.0 software. Specifically, classified and continuous variables were tested by Chi-square test and Student's t-test, respectively. The Kaplan-Meier method was employed to evaluate the survival time of OSCC patients based on median circ-MMP9 expression value. The correlation between circ-MMP9 and MMP9 expression was determined by Spearman's correlation coefficient. A p value less than 0.05 is considered statistically different.

Results

Circ-MMP9 is Overexpressed in OSCC and Positively Correlated with MMP9 Expression

Through the analysis of circBase database, we found that MMP9 can form three circRNAs: hsa_circ_0001161, hsa_circ_0060571, and hsa_circ_0001162 (circ-MMP9). We then assessed the expression levels of these three circRNAs in 74 paired tissues. As shown in Figure 1(a), only circ-MMP9 was significantly upregulated in OSCC tissues in comparison to adjacent normal tissues. Similar results were also observed in OSCC cell lines, especially in UM1 and HSC-3 cells with highly metastatic capacity (Figure 1(b)). Further, we found that circ-MMP9 expression was closely related to lymph node metastasis ($p=0.002$) and clinical TNM stage ($p=0.005$), but not to age, gender, tumor size, or site (Table 1). OSCC patients with high circ-MMP9 had a shorter overall survival time than those with low circ-MMP9 (Figure 1(c)). To test the diagnostic utility of circ-MMP9 in OSCC, we collected plasma samples from 16 healthy control and 25 OSCC patients to perform qRT-PCR. Consistently, circ-MMP9 was notably increased in OSCC plasma compared with healthy controls (Figure 1(d)), and the area under curve value was 0.91

Table 1. Association of circular matrix metalloproteinase 9 (circ-MMP9) expression with clinical parameters in 74 patients with oral squamous cell carcinoma (OSCC).

Parameters	Total ($n=74$)	circ-MMP9 expression Low ($n=37$)	circ-MMP9 expression High ($n=37$)	p value
Age (years)				
≤ 60	21	11	10	0.797
> 60	53	26	27	
Sex				
Male	36	15	21	0.163
Female	38	22	16	
Tumor site				
Tongue	58	28	30	0.311
Cheek	6	2	4	
Mouth floor	10	7	3	
T classification				
T1–T2	39	22	17	0.244
T3–T4	35	15	20	
Lymph node metastasis				
Negative	41	27	14	0.002
Positive	33	10	23	
TNM stage				
I–II	38	25	13	0.005
III–IV	36	12	24	

circ-MMP9: circular matrix metalloproteinase 9.

(95% confidence interval: 0.8216–0.9984) (Figure 1(e)), suggesting that plasma circ-MMP9 has high efficacy to distinguish between OSCC patients and healthy control. We then selected UM1 and HSC-3 cells to establish stable circ-MMP9 knockdown cell lines. As shown in Figure 1(f) and (g), depletion of circ-MMP9 dramatically reduced MMP9 mRNA as well as protein expression. In addition, high MMP9 expression was also observed in OSCC tissues as compared with paracancerous tissue (Figure 1(h)). Spearman's correlation coefficient result showed there was a strong positive correlation between circ-MMP9 and MMP9 expression in OSCC tissues ($r=0.719$, $p<0.001$) (Figure 1(i)). Altogether, these data indicate that circ-MMP9 is an effective prognostic and prognostic biomarker for OSCC patients, and it regulates the expression of its host gene.

Knockdown of Circ-MMP9 Inhibits OSCC Cell Migration and Invasion Both in vitro and in vivo

Next, we explored the biological function of circ-MMP9 in OSCC. The wound healing assay showed the migration distance of UM1 and HSC-3 cells was significantly shortened after knockdown of circ-MMP9 (Figure 2(a)). Likewise, the number of circ-MMP9-depleted UM1 and HSC-3 cells crossing the Matrigel was less than that of control cells (Figure 2(b)). Further, we established a lung metastasis model via tail-vein injection of UM1 cells into nude mice (Figure 2(c)). The
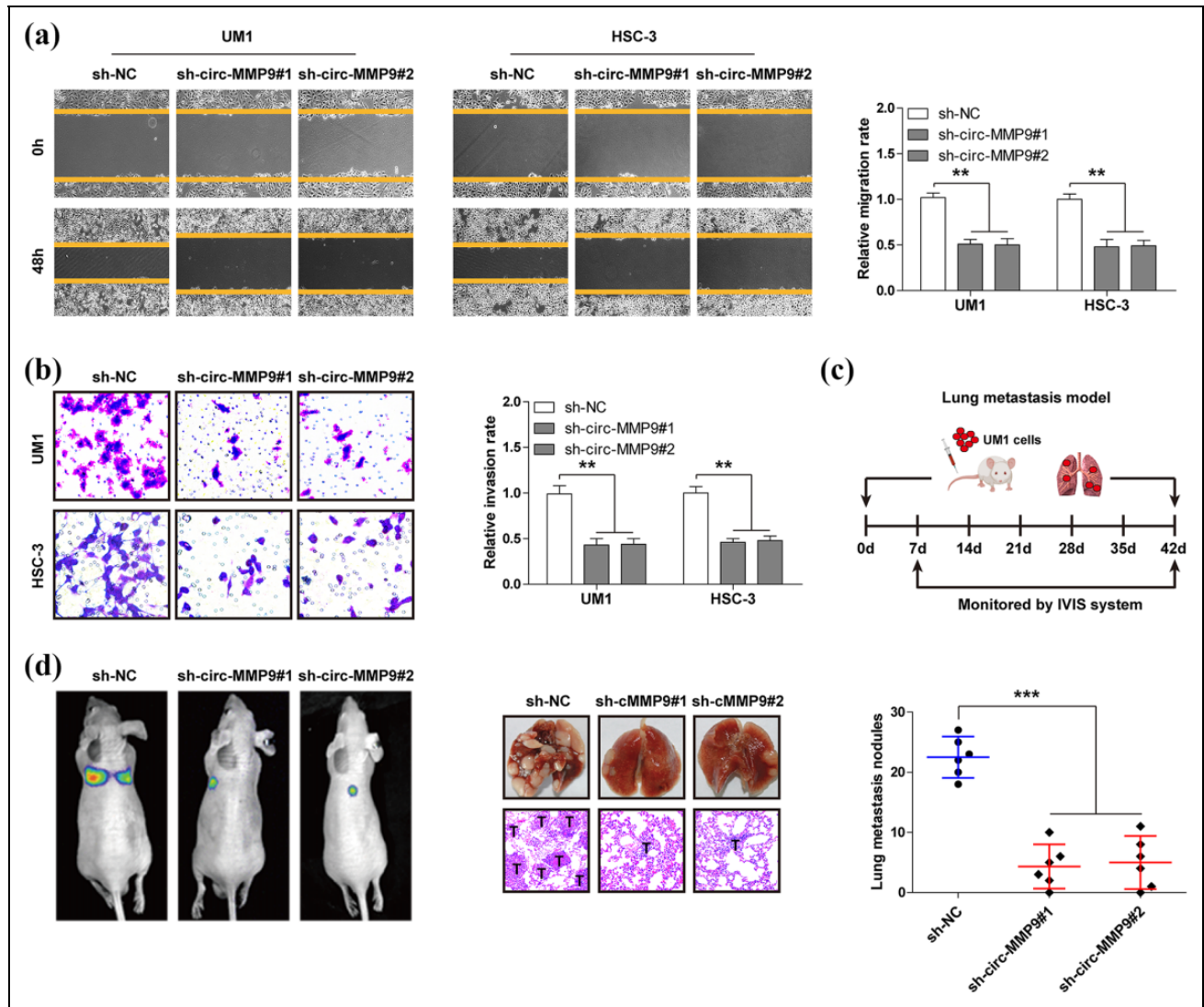
Fig 2. Circular matrix metalloproteinase 9 (circ-MMP9) depletion inhibits oral squamous cell carcinoma (OSCC) cell migration and invasion in vitro as well as lung metastasis in vivo. (a) Wound healing assay in circ-MMP9-depleted UM1 and HSC-3 cells. (b) Transwell invasion assay in circ-MMP9-depleted UM1 and HSC-3 cells. (c) A schematic diagram showing the specific process of establishing a lung metastasis model. (d) Representative images showing lung metastasis in vivo monitored by the IVIS system (left), lung tissues, and hematoxylin and eosin staining (middle) in the indicated three groups. The bold T denotes tumor. $**p < 0.01$, $***p < 0.001$.

results showed that an average of 23 lung metastatic nodules were observed in the control group, whereas only five were observed in circ-MMP9-depleted groups (Figure 2(d)). Overall, these in vitro and in vivo results suggest that circ-MMP9 is a pro-metastasis circRNA in OSCC.

Circ-MMP9 Directly Binds to AUF1 in OSCC

To test how circ-MMP9 affects MMP mRNA expression level, we first analyzed the promoter activity of MMP9. As shown in Figure 3(a), knockdown of circ-MMP9 had no effect on MMP9 promoter activity, implying that circ-MMP9 regulates MMP9 expression at a post-transcriptional level. We then treated UM1 and HSC-3 cells with Actinomycin D (a transcriptional inhibitor) to assess MMP9 mRNA stability. The results showed that circ-MMP9 depletion shortened the half-life of MMP9 mRNA by about 2 hours (Figure 3(b)). Given that AUF1 is a key regulator of mRNA stability[13] and the sequence alignment result showed there was an AUF1 binding motif ((A/U)UUU(A/U)) on MMP9 mRNA 3′-UTR (Figure 3(c)), we thus reasoned that AUF1 may be involved in the regulation of circ-MMP9 on MMP9. As expected, silencing AUF1 could significantly rescue the decreased MMP9 mRNA expression caused by circ-MMP9 depletion (Figure 3(d)). Through analyzing the RPISeq online
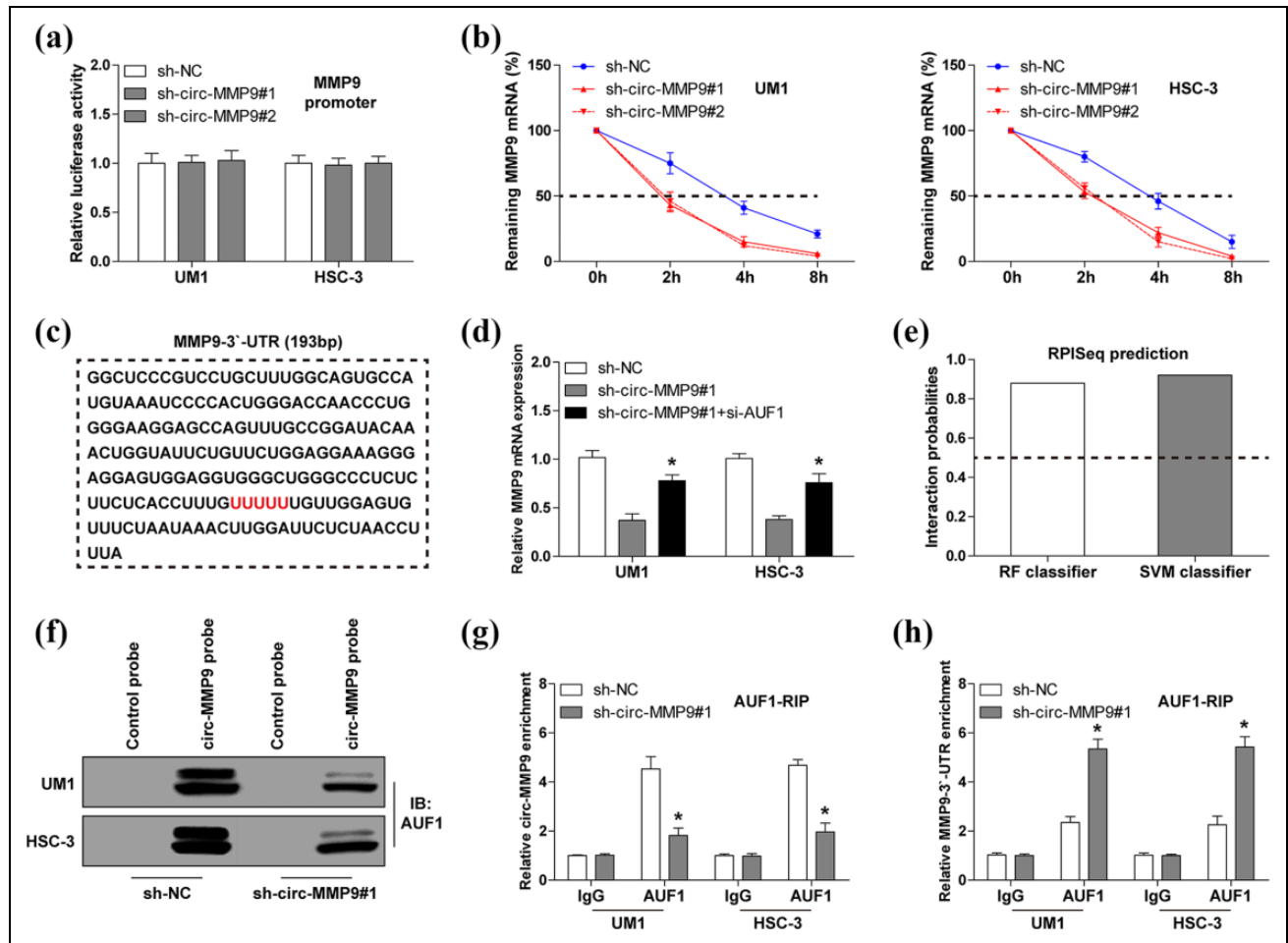
Fig 3. Circular matrix metalloproteinase 9 (circ-MMP9) stabilizes MMP9 messenger RNA (mRNA) via interaction with AUF1 in oral squamous cell carcinoma (OSCC) cells. (a) Luciferase reporter assay analysis for MMP9 promoter activity in circ-MMP9-depleted UM1 and HSC-3 cells. (b) Quantitative real-time PCR (qRT-PCR) analysis for MMP9 expression at the indicated time in circ-MMP9-depleted UM1 and HSC-3 cells treated with Actinomycin D. (c) The sequence marked in red denotes AUF1 binding motif on MMP9 3'-untranslated region (UTR). (d) qRT-PCR analysis for MMP9 expression in circ-MMP9-depleted UM1 and HSC-3 cells after transfection with si-AUF1. (e) The interaction probability between circ-MMP9 and AUF1 was predicted using RPISeq online tool, RF, and SVM classifier values > 0.5 were considered 'positive'. (f) RNA pull-down assay using biotin-labeled circ-MMP9 probe in UM1 and HSC-3 cells, followed by Western blot analysis for AUF1 expression. (g, h) Radioimmunoprecipitation assay using anti-AUF1 antibody in UM1 and HSC-3 cells, followed by qRT-PCR analysis for the enrichment of circ-MMP9 and MMP9 3'-UTR. $*p < 0.05$.

tool, we found that circ-MMP9 probably interacted with AUF1 (RF classifier=0.88, SVM classifier=0.91) (Figure 3(e)). This prediction was confirmed by the RNA pull-down assay, circ-MMP9 probe could abundantly enrich AUF1 protein, and the enrichment effect was weakened after circ-MMP9 knockdown (Figure 3(f)). A similar result was observed in RIPA using anti-AUF1 antibody (Figure 3(g)). However, circ-MMP9 knockdown did not affect AUF1 expression (data not shown). Importantly, depletion of circ-MMP9 remarkably increased the interaction between AUF1 and MMP9 3'-UTR (Figure 3(h)). Taken together, these findings demonstrate that circ-MMP9 enhances MMP9 mRNA stability via antagonizing AUF1-induced MMP9 mRNA decay in OSCC.

Circ-MMP9 Acts as a Sponge for miR-149 in OSCC

As mentioned above, AUF1 silencing could only partially rescue the reduced MMP9 mRNA caused by circ-MMP9 knockdown (Figure 3(d)), suggesting there are other factors mediating the regulation of circ-MMP9 on MMP9. We then determined the subcellular localization of circ-MMP9—the qRT-PCR and FISH results showed that circ-MMP9 was mainly localized in the cytoplasm (Figure 4(a) and (b)), which is consistent with its post-transcriptional regulation of MMP9. Numerous studies have reported that cytoplasmic circRNA can sponge microRNA (miRNA) to regulate gene expression[14], we thus searched for miRNAs with both circ-MMP9 and MMP9 binding sites using CircInteractome and miRanda databases, and the results showed that only miR-
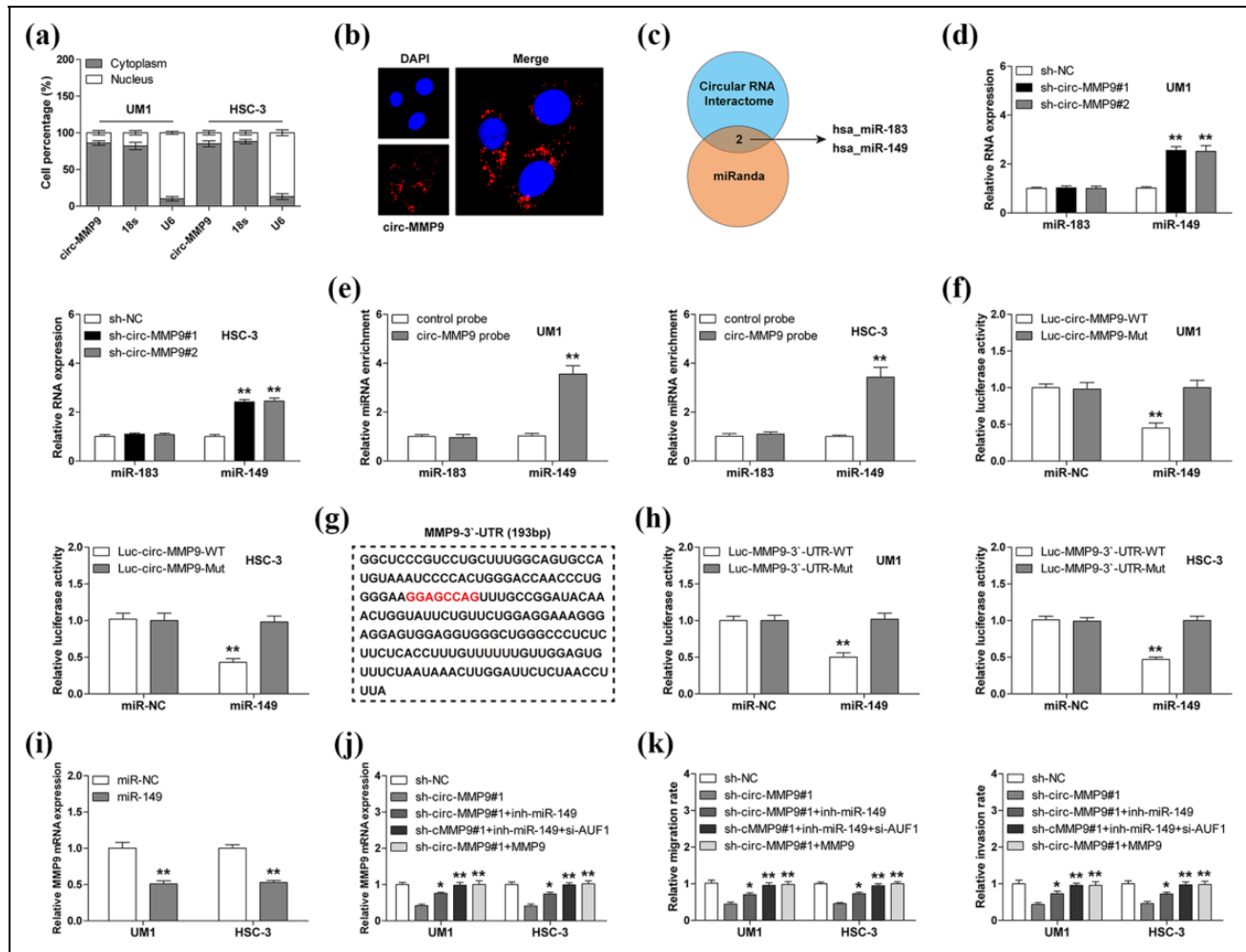
Fig 4. Circular matrix metalloproteinase 9 (circ-MMP9) sponges miR-149 in oral squamous cell carcinoma (OSCC) cells. (a, b) Quantitative real-time PCR (qRT-PCR) and fluorescence in situ hybridization (FISH) assays for the determination of cell sublocalization of circ-MMP9. Respectively, 18 s and U6 represented the internal references of cytoplasmic and nuclear fractions, and nucleus was stained by 4',6-diamidino-2-phenylindole. (c) microRNAs (miRNAs) with both circ-MMP9 and MMP9 binding sites predicted by CircInteractome and miRanda databases. (d) qRT-PCR analysis for miR-183 and miR-149 expression in circ-MMP9-depleted UM1 and HSC-3 cells. (e) RNA pull-down assay using biotin-labeled circ-MMP9 probe in UM1 and HSC-3 cells, followed by qRT-PCR analysis for miR-183 and miR-149 expression. (f) Luciferase reporter assay in UM1 and HSC-3 cells co-transfected with control or miR-149 mimics and wild-type or mutant circ-MMP9 reporter. (g) The sequence marked in red denotes miR-149 binding motif on MMP9 3′-untranslated region (UTR). (h) Luciferase reporter assay in UM1 and HSC-3 cells co-transfected with control or miR-149 mimics and wild-type or mutant MMP9 3′-UTR reporter. (i) qRT-PCR analysis for MMP9 expression in UM1 and HSC-3 cells transfected with control or miR-149 mimics. (j) qRT-PCR analysis for MMP9 expression in circ-MMP9-depleted UM1 and HSC-3 cells transfected with miR-149 inhibitors, miR-149 inhibitors+si-USF1, or MMP9 expression vector. (k) The assessment of migratory and invasive abilities of circ-MMP9-depleted UM1 and HSC-3 cells transfected with miR-149 inhibitors, miR-149 inhibitors+si-USF1, or MMP9 expression vector. $*p < 0.05$, $**p < 0.01$.

183 and miR-149 met this criterion (Figure 4(c)). As shown in Figure 4(d), circ-MMP9 depletion evidently upregulated the expression of miR-149, but not miR-183. Similarly, RNA pull-down results displayed that miR-149 rather than miR-138 was abundantly enriched by circ-MMP9 probe (Figure 4(e)). And miR-149 overexpression significantly reduced the luciferase activity of wild-type circ-MMP9 reporter, although it did not affect that of mutant reporter (Figure 4(f)). These results indicate that circ-MMP9 can sponge miR-149 in OSCC cells. Next, we tested whether

miR-149 could target MMP9. The sequence alignment result showed the binding site of miR-149 on MMP9 3′-UTR did not overlap with AUF1 (Figure 4(g)). The luciferase activity of wild-type MMP9 3′-UTR reporter rather than the mutated one was dramatically decreased after miR-149 overexpression (Figure 4(h)). And MMP9 mRNA expression was significantly downregulated in miR-149-overexpressing UM1 and HSC-3 cells (Figure 4(i)). Importantly, the decreased MMP9 mRNA and the attenuated migratory and invasive abilities caused by circ-MMP9 depletion were partly blocked
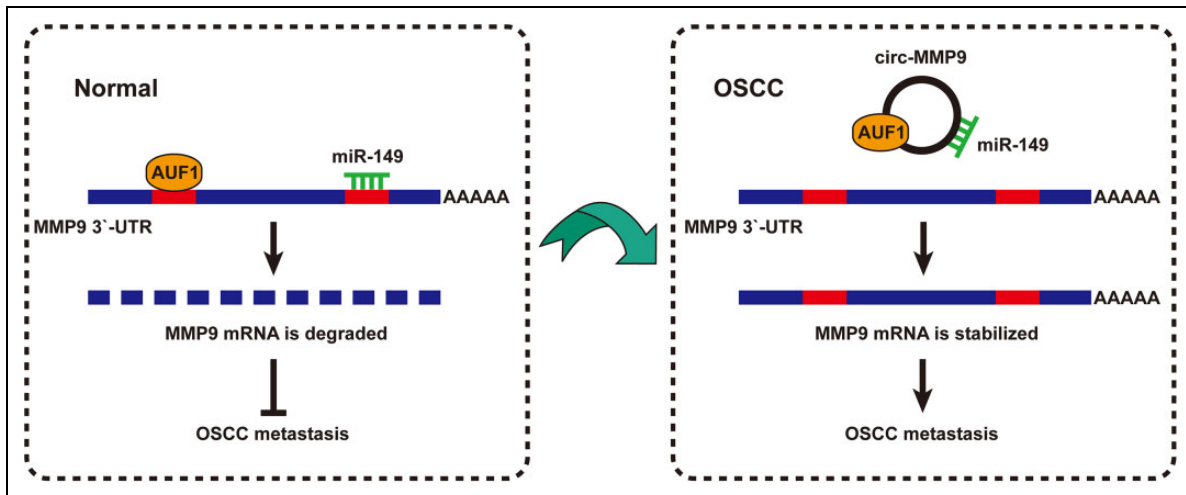
Fig 5. The proposed model of circular matrix metalloproteinase 9 (circ-MMP9) in promoting oral squamous cell carcinoma (OSCC) metastasis through interacting with miR-149 and AUF1 and enhancing MMP9 messenger RNA (mRNA) stability.

by miR-149 silencing, and were totally abolished by MMP9 overexpression or miR-149 silencing combined with AUF1 knockdown (Figure 4(j) and (k)). Collectively, these data suggest circ-MMP9 promotes OSCC metastasis through regulating its parental gene stability via miR-149 and AUF1 (Figure 5).

Discussion

Cancer metastasis is responsible for 90% of cancer-related deaths. Understanding the mechanism of metastasis is essential for identifying novel therapeutic targets. In the current study, we identified an OSCC metastasis-associated circRNA, referred to as circ-MMP9, which was markedly upregulated in OSCC tissues, plasma, and cell lines and closely correlated with poor outcome. Stepwise investigations revealed that circ-MMP9 could physically bind to AUF1 and miR-149 to protect MMP9 mRNA from degradation, leading to increasing MMP9 expression and facilitating OSCC invasion and metastasis. More importantly, knockdown of circ-MMP9 significantly suppressed the metastatic capability of OSCC cells in animal models, implying that therapeutic targeting of circ-MMP9 may be a promising treatment intervention for patients with metastatic OSCC.

As a class of endogenous non-coding RNA, circRNA has attracted great attention due to its unique loop structure and high stability and conservativeness. A large number of studies have shown that circRNA is aberrantly expressed in human cancers and plays a crucial role in cancer occurrence and development[15]. CircRNA functions through a variety of mechanisms, most notably as a molecular sponge for miRNAs, in which it abundantly absorbs miRNAs to alleviate inhibition of miRNAs on their target genes[16]. For example, circ-HIPK3[17], circ-ZEB1.33[18], circ-100146[19], and circ-ANKS1B[20] could effectively sponge miR-7, miR-200a-3p, miR-615-5p, miR-148/152, and miR-646 in colorectal

cancer, hepatocellular carcinoma, non-small cell lung carcinoma, and breast cancer, respectively. Herein, we found that circ-MMP9 was able to interact with miR-149 to elevate MMP9 expression in OSCC. Intriguingly, a recent study also identified circ-MMP9 as an oncogene that contributed to glioblastoma multiforme cell tumorigenesis via sponging miR-124[21]. However, our results showed that circ-MMP9 did not bind to miR-124 in OSCC (data not shown), although this discrepancy can be explained by the tissue and developmental-stage specific biological role of circRNA[22].

Another important mechanism by which circRNA functions is interaction with proteins. For instance, circ-Amotl1 was reported to directly bind to oncogene c-Myc to induce c-Myc nuclear translocation, thereby promoting tumorigenesis[23]. Circ-UBR5 could concurrently interact with QKI, NOVA1, and U1 small nuclear RNA in the nucleus to participate in the non-small cell lung cancer differentiation process[24]. Circ-Sirt1 was capable of inactivating NF-κB signaling via interacting with p65 and blocking p65 nuclear translocation[25]. In the present study, we found that circ-MMP9 could physically bind to AUF1 to increase MMP9 mRNA stability. AUF1 is a well-known mRNA destabilizer that targets the '(A/U)UUU(A/U)' motif on gene mRNA 3′-UTR[26]. Of note, the binding sites of AUF1 and miR-149 on MMP9 mRNA 3′-UTR did not overlap, suggesting they independently function to degrade MMP9 mRNA. A recent study proposed that circ-DNMT1 could also interact with AUF1 to reduce DNMT1 mRNA decay, resulting in facilitated breast cancer progression[27], and our data showed that depletion of circ-MMP9 enhanced the interaction between AUF1 and MMP9 mRNA; these findings indicate that circRNA plays a pivotal role in AUF1 regulation of mRNA stability.

In summary, our study clearly demonstrates that circ-MMP9 is a positive regulator of OSCC metastasis, and

highlights its important role in controlling the stability of MMP9 mRNA via AUF1 and miR-149, supporting the pursuit of circ-MMP9 as a potential treatment intervention for metastatic OSCC patients.

ORCID iD

Tao Hong ![ORCID] https://orcid.org/0000-0003-0974-6880

References

1. Chi AC, Day TA, Neville BW. Oral cavity and oropharyngeal squamous cell carcinoma–an update. CA Cancer J Clin. 2015; 65(5):401–21.

2. Bray F, Ferlay J, Soerjomataram I, Siegel RL, Torre LA, Jemal A. Global cancer statistics 2018: GLOBOCAN estimates of incidence and mortality worldwide for 36 cancers in 185 countries. CA Cancer J Clin. 2018;68(6):394–424.

3. Bossi P, Miceli R, Locati LD, Ferrari D, Vecchio S, Moretti G, Denaro N, Caponigro F, Airoldi M, Moro C, Vaccher E, et al. A randomized, phase 2 study of cetuximab plus cisplatin with or without paclitaxel for the first-line treatment of patients with recurrent and/or metastatic squamous cell carcinoma of the head and neck. Ann Oncol. 2017;28(11):2820–6.

4. Fridman R. Preface - Matrix metalloproteinases. Biochim Biophys Acta Mol Cell Res. 2017;1864(11 Pt A):1925–6.

5. Nishio K, Motozawa K, Omagari D, Gojoubori T, Ikeda T, Asano M, Gionhaku N. Comparison of MMP2 and MMP9 expression levels between primary and metastatic regions of oral squamous cell carcinoma. J Oral Sci. 2016;58(1):59–65.

6. Inaba H, Sugita H, Kuboniwa M, Iwai S, Hamada M, Noda T, Morisaki I, Lamont RJ, Amano A. Porphyromonas gingivalis promotes invasion of oral squamous cell carcinoma through induction of proMMP9 and its activation. Cell Microbiol. 2014;16(1):131–45.

7. Nanda DP, Dutta K, Ganguly KK, Hajra S, Mandal SS, Biswas J, Sinha D. MMP-9 as apotential biomarker for carcinoma of oral cavity: astudy ineastern India. Neoplasma. 2014;61(6): 747–57.

8. Kristensen LS, Hansen TB, Veno MT, Kjems J. Circular RNAs in cancer: opportunities and challenges in the field. Oncogene. 2018;37(5):555–65.

9. Eger N, Schoppe L, Schuster S, Laufs U, Boeckel JN. Circular RNA splicing. Adv Exp Med Biol. 2018;1087:41–52.

10. Li X, Wang J, Zhang C, Lin C, Zhang J, Zhang W, Zhang W, Lu Y, Zheng L, Li X. Circular RNA circITGA7 inhibits colorectal cancer growth and metastasis by modulating the Ras pathway and upregulating transcription of its host gene ITGA7. J Pathol. 2018;246(2):166–79.

11. Chen N, Zhao G, Yan X, Lv Z, Yin H, Zhang S, Song W, Li X, Li L, Du Z, Jia L, et al. A novel FLI1 exonic circular RNA promotes metastasis in breast cancer by coordinately regulating TET1 and DNMT1. Genome Biol. 2018;19(1):218.

12. Wu N, Yuan Z, Du KY, Fang L, Lyu J, Zhang C, He A, Eshaghi E, Zeng K, Ma J, Du WW, et al. Translation of yes-associated protein (YAP) was antagonized by its circular RNA via suppressing the assembly of the translation initiation machinery. Cell Death Differ. 2019.

13. White EJ, Matsangos AE, Wilson GM. AUF1 regulation of coding and noncoding RNA. Wiley Interdiscip Rev RNA. 2017;8(2):e1393.

14. Zhong Y, Du Y, Yang X, Mo Y, Fan C, Xiong F, Ren D, Ye X, Li C, Wang Y, Wei F, et al. Circular RNAs function as ceRNAs to regulate and control human cancer progression. Mol Cancer. 2018;17(1):79.

15. Shang Q, Yang Z, Jia R, Ge S. The novel roles of circRNAs in human cancer. Mol Cancer. 2019;18(1):6.

16. Chan JJ, Tay Y. Noncoding RNA: RNA regulatory networks in cancer. Int J Mol Sci. 2018;19(5):1310.

17. Zeng K, Chen X, Xu M, Liu X, Hu X, Xu T, Sun H, Pan Y, He B, Wang S. CircHIPK3 promotes colorectal cancer growth and metastasis by sponging miR-7. Cell Death Dis. 2018;9(4):417.

18. Gong Y, Mao J, Wu D, Wang X, Li L, Zhu L, Song R. Circ-ZEB1.33 promotes the proliferation of human HCC by sponging miR-200a-3p and upregulating CDK6. Cancer Cell Int. 2018;18:116.

19. Chen L, Nan A, Zhang N, Jia Y, Li X, Ling Y, Dai J, Zhang S, Yang Q, Yi Y, Jiang Y. Circular RNA 100146 functions as an oncogene through direct binding to miR-361-3p and miR-615-5p in non-small cell lung cancer. Mol Cancer. 2019; 18(1):13.

20. Zeng K, He B, Yang BB, Xu T, Chen X, Xu M, Liu X, Sun H, Pan Y, Wang S. The pro-metastasis effect of circANKS1B in breast cancer. Mol Cancer. 2018;17(1):160.

21. Wang R, Zhang S, Chen X, Li N, Li J, Jia R, Pan Y, Liang H. EIF4A3-induced circular RNA MMP9 (circMMP9) acts as a sponge of miR-124 and promotes glioblastoma multiforme cell tumorigenesis. Mol Cancer. 2018;17(1):166.

22. Ebbesen KK, Kjems J, Hansen TB. Circular RNAs: identification, biogenesis and function. Biochim Biophys Acta. 2016; 1859(1):163–8.

23. Yang Q, Du WW, Wu N, Yang W, Awan FM, Fang L, Ma J, Li X, Zeng Y, Yang Z, Dong J, et al. A circular RNA promotes tumorigenesis by inducing c-myc nuclear translocation. Cell Death Differ. 2017;24(9):1609–20.

24. Qin M, Wei G, Sun X. Circ-UBR5: an exonic circular RNA and novel small nuclear RNA involved in RNA splicing. Biochem Biophys Res Commun. 2018;503(2):1027–34.

25. Kong P, Yu Y, Wang L, Dou YQ, Zhang XH, Cui Y, Wang HY, Yong YT, Liu YB, Hu HJ, Cui W, et al. Circ-Sirt1 controls NF-kappaB activation via sequence-specific interaction and enhancement of SIRT1 expression by binding to miR-132/212 in vascular smooth muscle cells. Nucleic Acids Res. 2019;47(7):3580–93.

26. Moore AE, Chenette DM, Larkin LC, Schneider RJ. Physiological networks and disease functions of RNA-binding protein AUF1. Wiley Interdiscip Rev RNA. 2014;5(4): 549–64.

27. Du WW, Yang W, Li X, Awan FM, Yang Z, Fang L, Lyu J, Li F, Peng C, Krylov SN, Xie Y, et al. A circular RNA circ-DNMT1 enhances breast cancer progression by activating autophagy. Oncogene. 2018;37(44):5829–42.